# MEASURING AND UNDERSTANDING THE GYPSY GUITAR

*Nelson Lee*

CCRMA

Stanford, CA

nalee@ccrma.stanford.edu

*Antoine Chaigne*

ENSTA

Palaiseau, FR

antoine.chaigne@ensta.fr

*Julius O. Smith III*

CCRMA

Stanford, CA

jos@ccrma.stanford.edu

*Kevin Arcas*

ENSTA

Palaiseau, FR

arcas@ensta.fr

## ABSTRACT

We present measurements made on the gypsy guitar. Our goals in performing such measurements are to help understand the factors behind the specific tonal characteristics of this landmark stringed instrument. The gypsy guitar, made by Selmer-Maccaferri and Busato, possesses a unique, bright, non-linear shiny tone. Starting with the improvisational mastermind of Django Reinhardt, the sounds of this instrument live to this day. We explore measurements made on a monochord and on a Selmer-Maccaferri copy guitar. We discuss analyses of the measurements in both the spectral and time domains. From the measurements made, not only does the construction of the guitar play an important role in the guitar's sound, but the gypsy-style picking technique used to achieve high-volume sounds without amplification, and the gypsy vibrato used to sustain and color a note, highly influence the guitar's sound.

## 1. INTRODUCTION

From its appearance, to its tone, the gypsy guitar falls in its own category of acoustic guitars. Special strings are used, the body is shaped differently than modern-day folk and classical guitars, the frets are larger and fatter, and the neck-scale is longer than most acoustic guitars. With all these characteristics, the gypsy guitar gives a tone that is highly distinctive of not only the instrument and time-period, but of the music of Django Reinhardt that continues to thrive today in festivals all over the world.

Unique are the strings and picks used with the guitar. Gypsy guitar strings popular in use today are Argentines, made by Savarez in France. The strings contribute greatly to the unique gypsy guitar tone. Its low gauge strings offer its player a brighter, more metallic tone, with an ease for creating a very distinct vibrato.

The picks Django Reinhardt used ranged from stones to coat buttons. Players today choose picks with similar characteristics: thick and heavy.

The gypsy guitar body was built to be played above a band. The sound-hole on the gypsy guitar took on typically two forms: a small oval-hole or a large D-hole. Images of these two different types are shown in Figures 1(a) and 1(b) respectively. In the gypsy jazz community, the rhythm guitarist usually plays a D-hole and the lead player an oval-hole. The oval-hole has a brighter, more piercing tone while the D-hole has a warmer milder tone. The resulting difference can be explained by the larger sound-hole on the D-hole, which gives the instrument a lower air resonance.

Before amplification, a guitar player had to muscle out volume to be heard. Guitarists at the time chose these guitars because they offered a cutting tone that could be heard over an entire rhythm section. If played with the proper technique, the gypsy guitar could be played as a lead instrument along-side even horn instruments as was done by Django.

The gypsy guitar, known in France as the manouche guitar, gained popularity in the late 1920's. Played by Django Reinhardt through the 30's, 40's and 50's, these original Selmer-Maccaferri guitars are highly-sought after. Furthermore, Django's legacy lives on, as the music is still alive and in full swing, gaining popularity with more and more luthiers devoting shops to producing copies of this guitar. In this paper, we present a broad range of measurements made on a Selmer-Maccaferri copy with a D-hole. The guitar used was made by John McKinnard and carries the D'ell Arte label, model Hommage. The guitar had a larger body than those of the original Selmers and Busatos, as modeled after the gypsy guitars made by the renowned luthier Jacques Favino.

Our hopes in exploring the physics and mechanics behind the gypsy guitar is to ultimately develop high-fidelity physical-models for synthesis. We believe that modeling such an instrument, along with the difficult technique required to play it properly, will push the frontiers of physical-modeling in acoustic guitar synthesis. Preliminary progress in synthesis will be presented at the end of this paper

## 2. MOTIVATION

In the Computer Music community, there is extensive prior work in modeling the guitar. Using Digital Waveguides [1] and popular methods for measuring excitation signals to drive string models [2] and input admittance at the bridge of acoustic guitars [3], there is a clear methodology on approaching and modeling the guitar. We adopt the approaches made in the literature in that we approach experiments in such a decomposition: the string, the bridge/body and the radiation of the guitar. As discussed in [1], there are many advantages in approaching the guitar in such a fashion. For example similar physical models can be used to model both an electric and acoustic guitar; the main difference being that the electric guitar has a solid-body whereas the acoustic has a hollow-body.

(a) Image of a gypsy guitar with a small oval-hole. (b) Image of a gypsy guitar with a large D-hole.

Figure 1: Images of two gypsy guitars: one with a D-hole the other with an oval-hole

We approach the task of understanding the factors behind the gypsy guitar sound by studying the guitar's individual components: the strings, the body and the way sound waves are radiated.

### 2.1. Synthesis and Measurements

In this section, we discuss the relationship between synthesis and measurements of the acoustic guitar. As described in [2], current models use extensions of the Karplus-Strong algorithm with commuted synthesis. An excitation signal characteristic of the guitar pluck is used to drive a Digital Waveguide, which models the solution to the wave equation on a vibrating string. The output of the Digital Waveguide is then convolved with a filter that models the admittance at the bridge/body. The resulting signal is then passed through a radiation filter that filters the output to represent sound propagation from one point to another in space.

Commuted synthesis simplifies the computation chain by storing multiple excitations convolved with the admittance filter. This can be done because the system is Linear Time Invariant (LTI).

We performed measurements on the gypsy guitar with this framework in mind. The motion of the string was first measured to isolate the movement of the string held by a rigid and pseudo-rigid end as is the case when the note on the guitar that is played is fretted. The same sensors were then used to measure the motion of the string on the guitar to capture the behavior of the string in two orthogonal planes. In doing so, the non-linear pitch-shift caused by the gypsy-plucking technique, was carefully observed and better understood.

Measurements were then performed to obtain the admittance of the guitar body. These experiments would calibrate the guitar body admittance filter. Lastly, experiments were performed in an anechoic chamber to understand isolated-point radiation properties of the gypsy guitar.

### 2.2. Gypsy Guitar Technique

The community of gypsy jazz players today is a small, but blooming one. The handing down and refining through family tradition over the last hundred years of musical tradition have made the
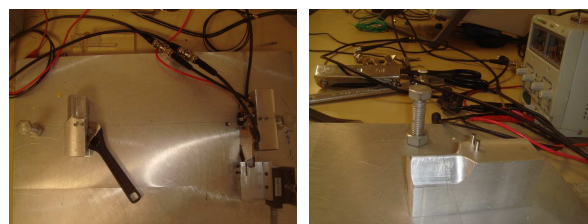


(a) Top-view of the monochord. (b) A close-up of the giving-end of the monochord

Figure 2: Photos of the monochord used.

technique required to play the gypsy guitar one of the most technically challenging in the world today.

Two important techniques are prevalent throughout the gypsy jazz community: the vibrato and plucking technique. The plucking technique, heavily influenced by Flamenco, allows a gypsy jazz guitar player to be heard above a band. When played correctly, it produces a cutting-tone with minimal effort. From a physical perspective, the plucking technique is the cause of the pitch-shift and many of the non-linearities heard in Django's old recordings. The pluck-hand is played freely, with minimal contact with the plate of the guitar. Furthermore, the pick displaces and releases the string quickly in the horizontal plane with the momentum of the plucking hand. Players today commonly use two millimeter Dunlop picks.

The other notable technique of Django's was his vibrato. With his left-hand, he was able to add color to his tone. Furthermore, by applying this technique, Django was able to sustain notes longer.

## 3. MEASUREMENTS AND PROCEDURE

In this section, we will present the various measurements performed. Again, as physical models decompose the guitar into components: the string, the bridge, the body and the radiation, we will present our methods and measurements broken down according to these components.

### 3.1. The String

To study the behavior of the string, we used two optoelectronic devices (H21B1), composed of a light emitting diode (LED) and a phototransistor, to record the displacement of the string at one point, close to the bridge, in two planes.

We first mounted the optoelectronic circuit for measurement on a monochord. The monochord used is shown in Figure 2(a). One end of the monochord was constructed to be as rigid as possible to prevent any transverse horizontal movement of the string. The other end was constructed to be used as two different ends: one rigid and one sliding. The sliding end was filed down to model the fret of a guitar.

The optoelectronic circuit was then placed within the soundhole of the gypsy guitar copy. Since the guitar used has a large D-shaped sound-hole, we drilled holes through the board, around soldered circuitry so that the guitar could be re-strung with all strings including the one being observed, passing through the board. Figure 3 shows an image of the optoelectronic circuit mounted on the actual guitar. As shown the string measured is the 'B' string as it passes through the two optoelectronic devices.
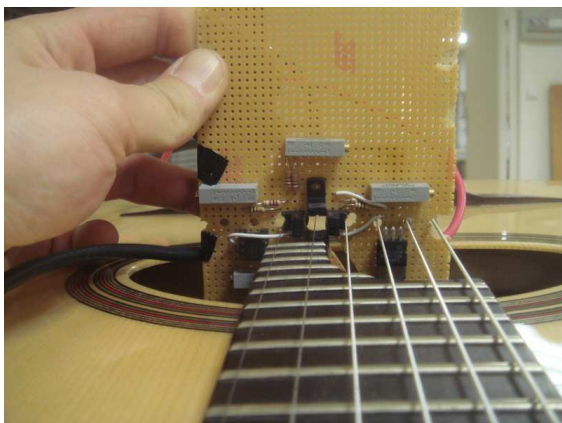
Figure 3: *The optoelectronic circuit mounted on the guitar. The strings of the guitar pass through the circuit; the 'B' string passes through the two optoelectronic devices.*

### 3.2. The Bridge

The gypsy guitar bridge is floating, meaning it is held in place by the strings of the guitar, similar to a violin bridge. Figure 4(a) shows a close-up of the gypsy guitar's bridge. We made measurements on the bridge by mounting a B&K shaker and impedance head to it. We input to the shaker white noise for approximately 100 seconds where the acceleration at the driving-point was recorded. Note though the shaker may affect the admittance below $200 - 300$Hz because of coupling with the moving coil, but its impact on higher frequencies is negligible. Furthermore, since such high-end equipment was used, good signal-to-noise ratio recordings were obtained.

### 3.3. Pressure Radiation

Measurements made to understand the way the gypsy guitar radiates its sound were made in an anechoic chamber. The guitar was placed on the ground in the room, with a shaker attached to its bridge. A B&K condenser microphone was placed above the guitar at varying distances. White noise was fed as input into the shaker. Both the accelerometer signal on the bridge and the signal from the condenser microphone were recorded. The experimental setup is shown in Figures 4(b) and 4(c).

### 3.4. Plate Vibration

To observe the modes of the top-plate of the guitar, a Polytec Vibrometer was used. Figure 4(d) shows the experimental setup of the vibrometer above the guitar. The Polytec vibrometer was setup above the guitar, pointing-down, to capture the transverse motion of the top-plate and bridge. The guitar was driven with white noise using the shaker from previous measurements. The white noise driving the shaker was fed into the vibrometer as the reference signal.

With the software provided from Polytec, we were able to view animations of the movement of the top-plate at frequencies within half the sampling-rate.



(a) close-up view of the gypsy guitar bridge.

(b) An image of the shaker, microphone and guitar setup in the anechoic chamber.

(c) A close-up of the shaker at the bridge in the anechoic chamber

(d) A close-up of the Vibrometer's laser on the guitar bridge.

Figure 4: Photos of experimental setups with the D-hole guitar

### 3.5. Comprehensive Measurements

In an attempt to capture the behavior of each modeled component simultaneously, we performed measurements that recorded six signals at one time. These signals include the two outputs from the optoelectronic circuit, as mounted on the guitar, the output of an accelerometer mounted on the bridge of the guitar, the output of a condenser microphone placed above the guitar, the output of a Big-Tone pickup, a pickup that is a microphone within the bridge itself, and the output of the vibrometer pointed at a point on the top-plate of the guitar close to the bridge. The guitar was placed on the ground and was plucked by a player in the genre of gypsy jazz using the gypsy guitar plucking technique. Thirty-two notes were measured on the guitar. Sixteen pitches on the 'B' string were made, starting with the open string up to the 15th fret. The same was done with the high 'E' string.

## 4. ANALYSIS

### 4.1. The String

Figures 5, 6, 7 and 8 show the measurements and corresponding analyses of the data recorded from the optoelectronic circuit mounted on the guitar and on the monochord. Plots in the left show time-domain amplitude plots of the horizontal plane, plots in the middle show time-domain amplitude plots of the vertical plane and plots in the right column show the frequencies of the fundamentals of each waveform. The spectral plots were obtained by sliding an FFT-window of length $2^{22}$ samples through each time-domain waveform.

#### 4.1.1. Pitch Shift

From our experiments, we were able to observe the pitch shift of a plucked note on the gypsy guitar. Shown in Figure 5, the fundamental at the onset is approximately 5Hz higher than the steady-

(a) Time-domain plot of horizontal plane  (b) Time-domain plot of vertical plane  (c) Spectral plot of pitch-shifting in both planes

(d) Time-domain plot of horizontal plane  (e) Time-domain plot of vertical plane  (f) Spectral plot of pitch-shifting in both planes

(g) Time-domain plot of horizontal plane  (h) Time-domain plot of vertical plane  (i) Spectral plot of pitch-shifting in both planes

Figure 5: Recordings using the optoelectronic circuit mounted onto the guitar. Figures on the left show the time-domain amplitudes of the horizontal moving waves. Figures in the middle show the time-domain amplitudes of the vertical moving waves. Figures on the right show the maximum amplitude frequency of the fundamental for both the horizontal and vertical planes. The top two rows are recordings and analyses of recordings made on the high 'E' string at the 10th and 11th frets. The third row shows the recording made at the 15th fret of the 'B' string.

(a) Time-domain plot of horizontal plane      (b) Time-domain plot of vertical plane      (c) Spectral plot of pitch-shifting in both planes



(d) Time-domain plot of horizontal plane      (e) Time-domain plot of vertical plane      (f) Spectral plot of pitch-shifting in both planes
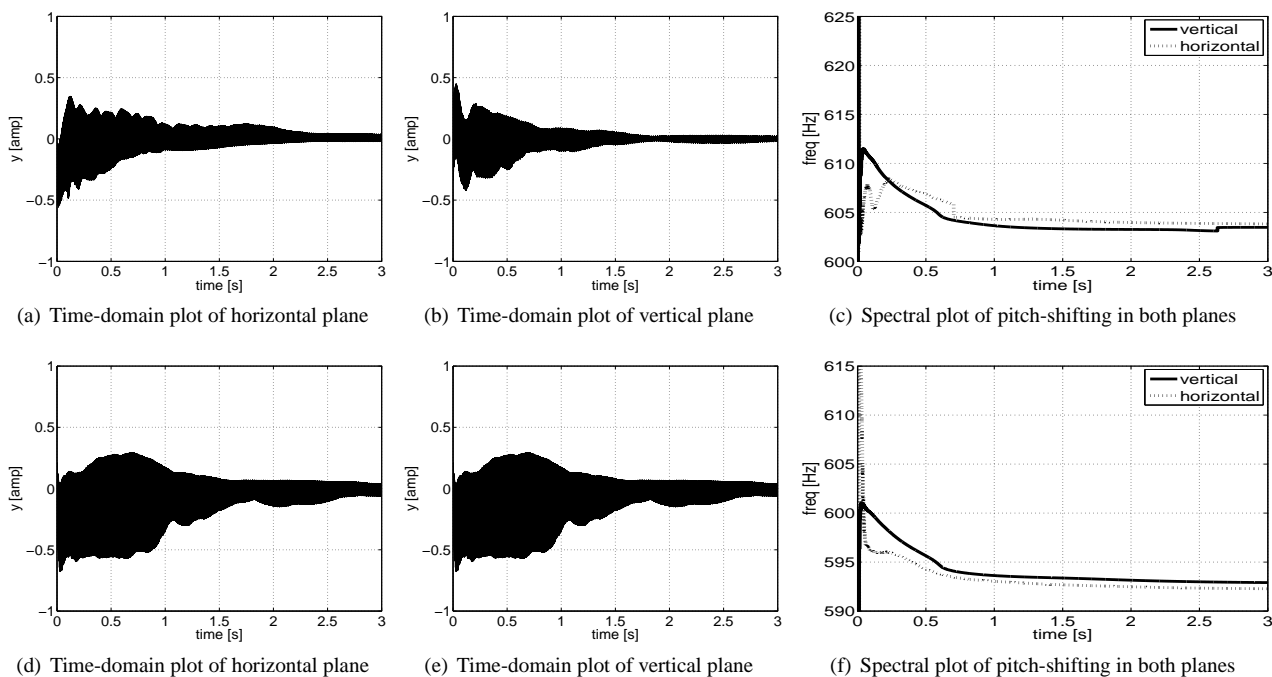
Figure 6: Recordings using the optoelectronic circuit mounted onto the monochord. Figures on the left show the time-domain amplitudes of the horizontal moving waves. Figures in the middle show the time-domain amplitudes of the vertical moving waves. Figures on the right show the maximum amplitude frequency of the fundamental for both the horizontal and vertical planes. The top row shows recordings and analyses of recordings made with the sliding end on the monochord, while the bottom row shows those with the rigid end on the monochord. Both plucks were heavy-forced plucks directed in the horizontal plane.



(a) Time-domain plot of horizontal plane      (b) Time-domain plot of vertical plane      (c) Spectral plot of pitch-shifting in both planes



(d) Time-domain plot of horizontal plane      (e) Time-domain plot of vertical plane      (f) Spectral plot of pitch-shifting in both planes
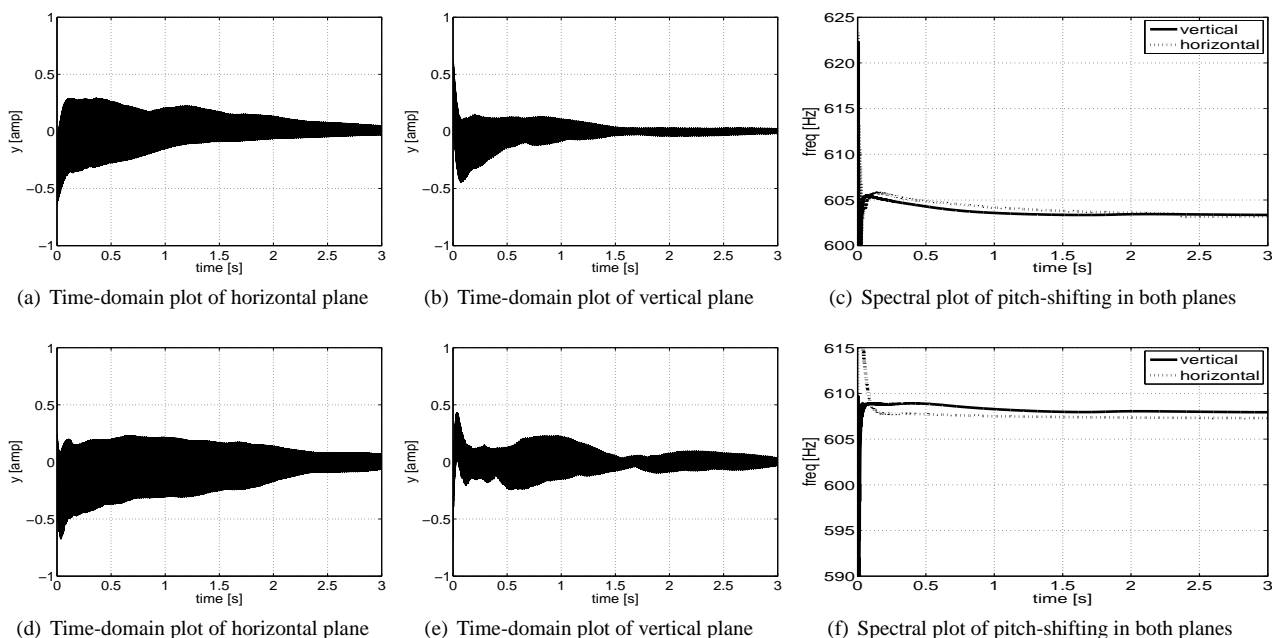
Figure 7: Recordings using the optoelectronic circuit mounted onto the monochord. Figures on the left show the time-domain amplitudes of the horizontal moving waves. Figures in the middle show the time-domain amplitudes of the vertical moving waves. Figures on the right show the maximum amplitude frequency of the fundamental for both the horizontal and vertical planes. The top row shows recordings and analyses of recordings made with the sliding end on the monochord, while the bottom row shows those with the rigid end on the monochord. Both plucks were medium-forced plucks directed in the horizontal plane.
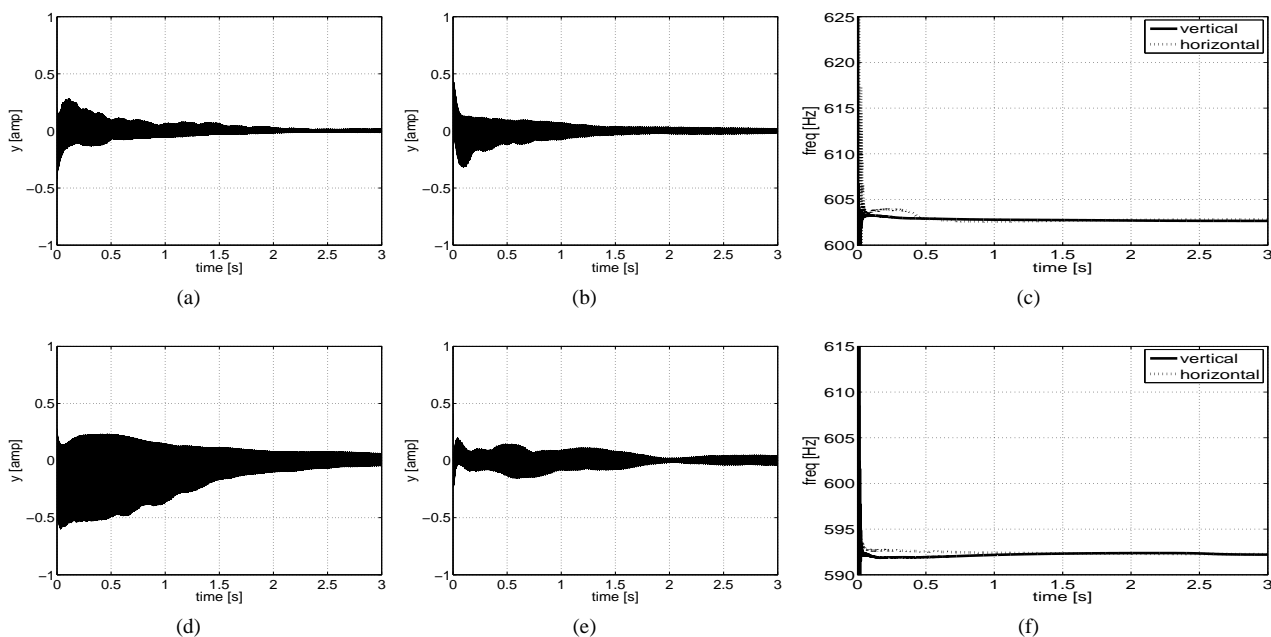
Figure 8: Recordings using the optoelectronic circuit mounted onto the monochord. Figures on the left show the time-domain amplitudes of the horizontal moving waves. Figures in the middle show the time-domain amplitudes of the vertical moving waves. Figures on the right show the maximum amplitude frequency of the fundamental for both the horizontal and vertical planes. The top row shows recordings and analyses of recordings made with the sliding end on the monochord, while the bottom row shows those with the rigid end on the monochord. Both plucks were light-forced plucks directed in the horizontal plane.

state frequency. Furthermore, in Figure 5, the horizontal plane is vibrating at a slightly higher frequency than that of the vertical plane even after the initial stretching of the string from the attack. This matches intuitively what happens when one is playing the gypsy guitar with the gypsy-picking technique: a heavy-forced horizontal displacement. Furthermore, this explains the beating effects heard when one plays the gypsy guitar.

This phenomenon is a common occurrence when playing the gypsy guitar. We want to emphasize the point that though most stringed instruments with one rigid and one sliding end can be made to display such pitch shifting when the string is set into motion with a high-enough displacement, this is, however, common for the gypsy guitar.

### 4.1.2. *Giving-end vs. Rigid-end*

Figures 6, 7 and 8 show time-domain amplitude plots of both planes and their corresponding fundamental frequency trackings for heavy-forced, medium-forced and light-forced plucks, respectively on the monochord. In Figure 6, it is clear that more non-linear behavior is observed with higher-force plucks for both the rigid end and giving end on the monochord. In Figure 8 the pitch-shifting effects are minimal. In examining giving-end data versus rigid-end data, the sliding-end exhibits more erratic behavior in the horizontal-plane in the fundamental tracking plots. This is not surprising since the sliding-end interacts much more intricately with the vibrating string than the rigid-end.

Comparing Figures 6(c) and 6(f), the prior plot, the one with the giving end, has discontinuities in its curve. Upon closer examination of the FFT for the corresponding waveform, the cause for

the discontinuities are two very close peaks in the corresponding waveform's FFT. The discontinuity that occurs at approximately 0.7 seconds, is due to the initial peak being tracked up to 606Hz having amplitude smaller at that point in time than the other peak at 605Hz. Therefore, the maximum-amplitude peak chosen was not the same as the peak our algorithm had been tracking before, thus causing the discontinuity. For future work, using a very large sliding FFT window as we have done and tracking numerous peaks in each plane, rather than selecting the maximum peak in each plane would divulge the way the string vibrates in the two orthogonal planes and how the motion in each plane is correlated with one another.

### 4.2. The Body

In this section we use measurements obtained in Section 3.2 to obtain the driving-point admittance at the bridge. The admittance is defined as follows:

$$\Gamma(\omega) = \frac{V(\omega)}{F(\omega)} \tag{1}$$

$$|\Gamma(\omega)| = \frac{|V(\omega)|}{|F(\omega)|} \tag{2}$$

$$\angle\Gamma(\omega)| = \angle|V(\omega)| - \angle|F(\omega)| \tag{3}$$

Figures 9(a) and 9(b) plot both the magnitude and phase of the admittance as defined in Equations 2 and 3, respectively.
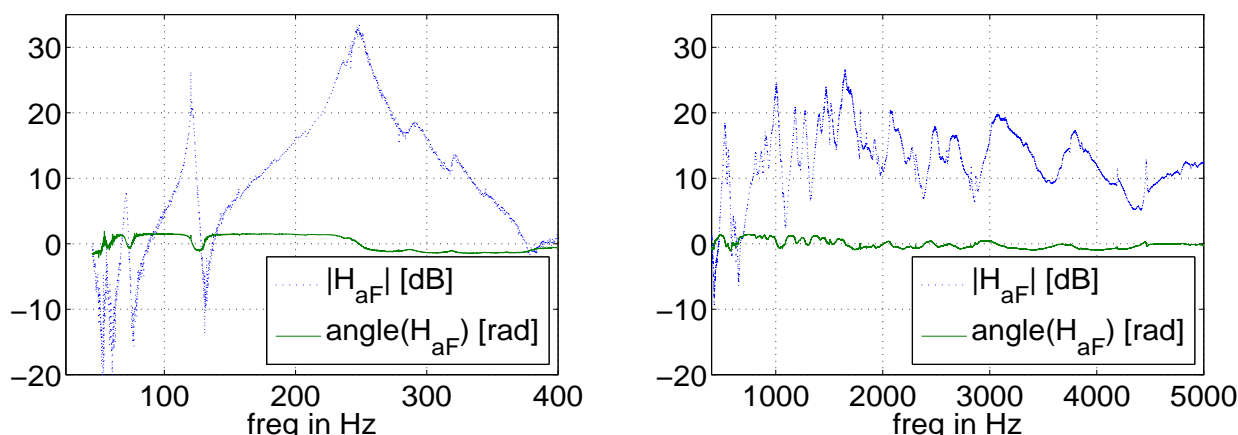
(a) The measured body response of the gypsy guitar. The plot is focused on the Air Resonant Frequency.

(b) The measured body response of the gypsy guitar. The plot is focused on modes above 1 kHz.

Figure 9: Plots of the driving-point admittance as measured at the bridge of the guitar.

### 4.2.1. The Air Resonance

In Figure 9(a), both the phase and magnitude curves show that the air resonant frequency occurs at 120 Hz. As Figure 9(a) shows, there are many prominent modes below one kilo-Hertz. The mode with the highest magnitude occurs close to 250 Hz.

One important characteristic of the gypsy guitar is that the top-plate resonates higher-frequencies greater than those of the top plate of classical guitars. Figure 9(b) shows a plot of the driving-point impedance of the gypsy guitar between 400 to 5000 Hz. This helps explain the bright, 'twangy' sound one hears from the gypsy guitar. Compared with the driving-point admittance of a classical guitar, at higher frequencies, the body of a classical guitar is much more rigid.

### 4.3. Radiation

We discuss measurements described in Section 3.3. With the recordings of the acceleration at the bridge and the pressure waves from the condenser microphone above it, we were able to compute the transfer function for the two. This aligns with our hopes of compartmentalizing the physical mechanisms of the guitar. However, we note that we are satisfied with synthesizing an acoustic guitar tone generated at one point and heard at one point in space.

### 5. SYNTHESIS

With the data collected, we can now psycho-acoustically fine tune parts of our guitar model that do not match what should actually be occurring physically. Below we describe the use of the data collected in the anechoic chamber as described in Section 3.3.

### 5.1. Calibrating the Radiation Filter

Figure 10(a) shows the computed transfer function from acceleration to pressure waves using the measurements taken from the experiment described in Section 3.3. As shown, there is a slant in the resulting spectrum giving a low-pass characteristic. Since our measurements in Section 3.5 measured the displacement of the string close to the bridge, the acceleration at the bridge and the pressure waves radiated from the guitar simultaneously, we judged the accuracy of our computed radiation filter by convolving it with our accelerometer measurements at the bridge. Since we had what the pressure waves were at that given recording of the accelerometer, we compared the true recording to the filtered signal. Not surprisingly, because of the low-pass characteristic of our radiation filter, the filtered signal lacked high-frequency components. To compensate for this low-pass characteristic while remaining true to the measured radiation filter's shape, the slant of the radiation filter into higher frequencies was removed. In doing so, psycho-acoustically similar tones to those recorded with the condenser microphone were obtained. Figure 10(b) shows the original transfer function and the resulting calibrated transfer function used for a radiation filter.

### 6. CONCLUSIONS

In this paper we present comprehensive measurements made on the gypsy guitar. Measurements are made with the intention of building and calibrating physically-based models for re-synthesis. Also presented are observations and measurements that give insight into what gives the gypsy guitar its unique tone. We show how to calibrate our synthesis models using real measured data. We explored the radiation filter component of our physical model using the measurements made to provide psycho-acoustically similar tones with those recorded from the actual guitar. Furthermore, we present a novel method for measuring the behavior of a vibrating string on the guitar: an optoelectronic circuit mounted on the guitar, and present analyses of differing non-linear behaviors in the horizontal and vertical vibrating planes of the string.

### 7. REFERENCES

[1] Julius O. Smith, *Physical Audio Signal Processing*, http://ccrma.stanford.edu/~jos/pasp/, Aug.

(a) The computed transfer function of pressure divided by acceleration.



(b) The calibrated transfer function between acceleration and pressure.
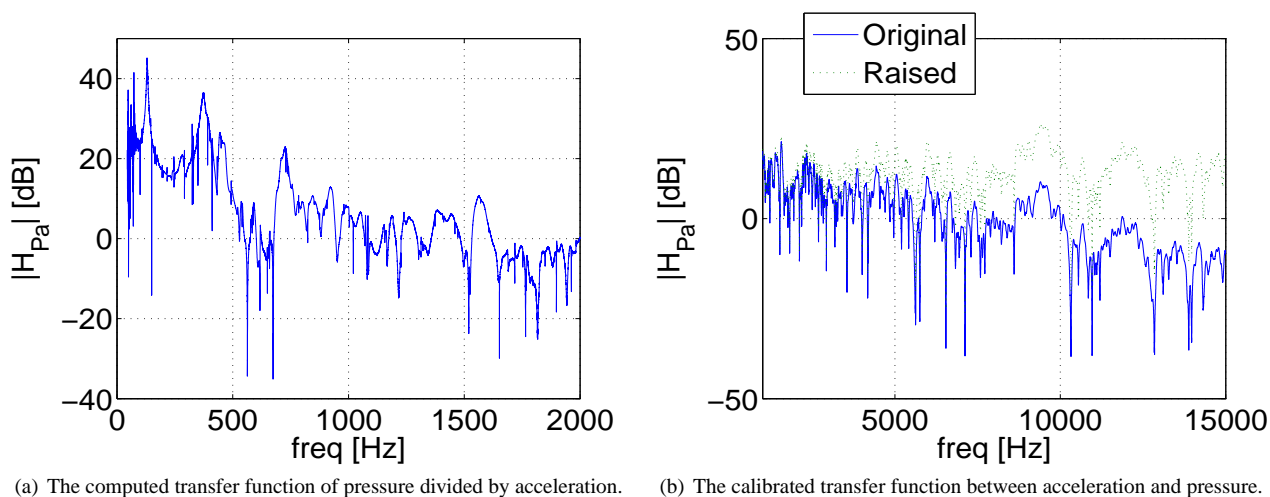
Figure 10: Measured radiation filter and calibrated radiation filter. In Figure 10(b), The solid line represents the unmodified transfer function. The dotted line shows the modified transfer function.

2006, online book.

[2] Tero. Tolonen, "Model-based analysis and resynthesis of acoustic guitar tones," M.S. thesis, Helsinki University of Technology, 1998.

[3] B.E. Richardson, T. J. W. Hill, and S.J. Richardson, "Input admittance and sound field measurements of ten classical guitars," in *Proceedings of the Institute of Acoustics*. 2002, vol. 24(2), pp. 1–10, IOA.

[4] X. Serra, *Musical Signal Processing*, chapter Musical Sound Modeling with Sinusoids plus Noise, pp. 91–122, G. D. Poli and A. Picialli and S. T. Pope and C. Roads Eds. Swets & Zeitlinger, 1996.

[5] A. Chaigne, "On the use of finite differences for the synthesis of musical transients. application to plucked stringed instruments," in *Journal d'Acoustique 5*, 1992, pp. 181–211.

[6] C. Lambourg and A. Chaigne, "Measurements and modeling of the admittance matrix at the bridge in guitars," in *Proceedings of the SMAC 93*, 1993, pp. 448–453.

[7] O. Christensen and R.B. Vistisen, "A simple model for low-frequency guitare function," *J. Acoust. Soc. Am.*, vol. 68, pp. 758–766, 1980.

[8] B. E. Richardson, "Simple models as a basis for guitar design," *Catgut Acoustica Society Journal*, vol. 4, no. 5, pp. 30–36, 2002.